Evaluating GPS Receiver Robustness to Ionospheric Scintillation

Joanna C. Hinks, *Cornell University*
Todd E. Humphreys, *Coherent Navigation*
Brady O'Hanlon, *Cornell University*
Mark L. Psiaki, *Cornell University*
Paul M. Kintner, Jr., *Cornell University*

BIOGRAPHY

Joanna C. Hinks is a Ph.D. student in Mechanical and Aerospace Engineering at Cornell University. Her research interests include estimation, spacecraft attitude and orbit determination, and GNSS technology.

Todd E. Humphreys is a research assistant professor in the department of Aerospace Engineering and Engineering Mechanics at the University of Texas at Austin. He will join the faculty of the University of Texas at Austin as an assistant professor in the Fall of 2009. He received a B.S. and M.S. in Electrical and Computer Engineering from Utah State University and his Ph.D. in Aerospace Engineering from Cornell University. His research interests are in estimation and filtering, GNSS technology, GNSS security, and GNSS-based study of the ionosphere and neutral atmosphere.

Brady O'Hanlon is a second year Ph.D. student in Electrical and Computer Engineering at Cornell University. His interests include GNSS technologies and space weather.

Mark L. Psiaki is a Professor in the Sibley School of Mechanical and Aerospace Engineering. He received a B.A. in Physics and M.A. and Ph.D. degrees in Mechanical and Aerospace Engineering from Princeton University. His research interests are in the areas of estimation and filtering, spacecraft attitude and orbit determination, and GNSS technology and applications.

Paul M. Kintner, Jr. is a professor of Electrical and Computer Engineering and a Fellow of the American Physical Society. He works at the intersection of space weather and GNSS.

ABSTRACT

A method for testing GPS receivers for ionospheric scintillation robustness has been implemented using a GPS signal simulator and a statistical model that captures the characteristics of scintillation relevant to receiver performance. This technique will help GNSS equipment manufacturers and users prepare for the approaching solar maximum by enabling repeatable receiver performance tests under realistic scintillation conditions. Ionospheric scintillation can impair the performance of phase tracking loops in GNSS receivers by introducing deep amplitude fades and abrupt phase changes in a signal. A statistical model has been developed that accurately recreates these effects by shaping the complex spectrum rather than treating phase and amplitude individually. Generated scintillation histories have been incorporated into the output of a GPS signal simulator so that any compatible receiver can be evaluated without modification. Such a hardware-in-the-loop approach provides a controlled test environment and the ability to characterize receiver performance statistically by running many experiments. It expands the range of possible test conditions beyond those available during field testing. The method is simple to implement, and its value has been demonstrated by a variety of tests applied to four different receivers.

I. INTRODUCTION

As GNSS signals propagate through the ionosphere, they may encounter irregularities in electron density. The resulting scattering and recombining of the radio waves is known as ionospheric scintillation, and it manifests at the receiver as rapid fluctuations in signal phase and power [1]. During severe scintillation, a receiver's phase lock loop (PLL) may have difficulty tracking the quickly varying carrier phase, or a deep power fade may cause the signal to drop below the noise floor. These effects result in cycle slips or even complete loss of lock [2,3] .

The most severe ionospheric scintillation occurs in equatorial regions, especially during periods of high solar activity. While it will not affect most GNSS users, scintillation could impact any application where extreme accuracy and reliability are paramount. For example, there is concern within the aviation community that severe scintillation effects may prevent modern GPS-based air traffic control systems from meeting their exacting integrity requirements. Such concerns will become more acute with the increased scintillation activity ushered in by the 2011 solar maximum.

It has been shown that, within a class of standard GNSS carrier tracking loops, certain tracking parameters can be tuned to maximize scintillation robustness [2,3]. Other, more exotic strategies involving data bit aiding or parity checking are even more effective [3]. Critical to the development of improved tracking strategies is the ability to test receiver performance under various severity levels of realistic scintillation.

When one thinks about testing a GNSS receiver for robustness to scintillation, there are several important considerations. First, investigations may be conducted at the level of software or mathematical receiver models, or the entire receiver hardware may be evaluated. By testing only the back end of the receiver using intermediate frequency (IF) data as in [4], one isolates the tracking loops and the consequences of loop design changes are obvious. However, this strategy avoids the effects of RF front end processing that are present in every commercial receiver. Tests of the full receiver including the RF front end, on the other hand, most accurately reflect typical receiver operation [5].

A second, related consideration for receiver testing is the source of scintillation data, which may be empirical or synthetic. Receivers may be tested in the field by measuring performance during real scintillation events [6], or scintillation data can be pre-recorded for future use [5,7]. Each technique subjects the receiver to actual scintillation without modeling errors. Empirical data use limits the investigation to scintillation for which data were recorded, however, and does not allow for either hypothetical test cases or for tests with long intervals of statistically stationary scintillation data. Synthetic scintillation, while providing such flexibility, requires extra caution to avoid modeling errors.

Models that generate synthetic scintillation come in several different forms. Physics-based ionospheric models often focus on predicting rather than generating scintillation [8,9], and require a large set of input parameters that do not necessarily relate to the tracking ability of a receiver. Phase screen models are simpler, but current forms still involve a more complex set of inputs

than is desirable for receiver tests [10]. Statistical models may be designed with a simple parameter set relevant to receiver tracking [4,6,10,11], but care must be taken to ensure that they accurately imitate empirical scintillation. Otherwise, users may be surprised to see actual receiver performance degradations much worse than those predicted by laboratory testing, as occurred in field testing on Ascension Island during the 2000 solar maximum [6]. A good statistical model of scintillation must capture all the characteristics of real scintillation that tend to disrupt PLL tracking capabilities, without necessarily addressing the physical processes that gave rise to those characteristics. Such a model has been developed in Reference [12] based on analysis of a large library of empirical scintillation data.

This paper proposes a simple yet effective method for scintillation robustness evaluation. It incorporates the previously developed realistic statistical scintillation model and a hardware-in-the-loop approach employing a GPS signal simulator. Such a combination enables testing of almost any hardware or software receiver, and allows great flexibility in the design of scintillation test scenarios. Furthermore, this strategy lends itself to comparisons between different receiver models, and to quantifiable performance characterization of a given receiver under varying levels of scintillation severity.

The scintillation test method is developed in three main sections plus conclusions. Section II describes the statistical scintillation model and the use of this model to generate time histories of synthetic scintillation. In Section III the hardware-in-the-loop procedure is developed, and its capabilities are explained. Section IV presents the results of method validation and receiver testing. Conclusions are presented in Section V.

II. GENERATION OF STATISTICAL SCINTILLATION

The statistical scintillation model advanced in Reference [12] was developed specifically to study GNSS carrier phase tracking. To that end, it is as simple as possible (in terms of number of parameters and ease of implementation), while still maintaining all the signal properties that tend to stress carrier tracking loops. A large library of empirical scintillation data [2] provides the model with its foundation in the physical world. An overview of some of the most important features of this model is presented in the next three paragraphs, followed by a more detailed description of the model statistics and implementation. Readers interested in the data analysis justifying the various design decisions should refer to Reference [12].

The model focuses exclusively on strong equatorial scintillation because it is the most difficult case for a receiver to track. It characterizes the scintillation time histories with just two parameters: S_4, the standard scintillation intensity index, and τ_0, the decorrelation time of the complex fading process. As S_4 increases, the power fades grow deeper and may even descend below the noise floor. Likewise, as τ_0 decreases (the peak of the autocorrelation function grows narrower), both phase and amplitude change more rapidly and thus become more difficult to track. Reference [3] further demonstrates how S_4, τ_0, and the signal carrier-to-noise ratio (C/N_0) can be used to obtain a rough estimate of T_s, the mean time between cycle slips.

In its current form this model only generates scintillation on one frequency at a time; properly correlated scintillation on multiple frequencies has not yet been implemented but is planned for future model versions. At present, the effects of multi-frequency scintillation can be bounded by applying cases of identical or independent data to a second frequency. For receivers that do not use data from one frequency to aid tracking at another frequency, the current model is sufficient.

An important and recurrent feature in time histories of strong scintillation has been termed a "canonical fade" by the authors. A canonical fade is said to occur when the signal simultaneously experiences a deep power fade and an abrupt phase change of approximately half a cycle. This situation is particularly challenging for PLL tracking because just when the phase is changing rapidly and most difficult to track, the signal level decreases and thus reduces the ability to accurately measure phase. Inspection has verified that the majority of cycle slips during strong scintillation can be linked to a canonical fade event. Although the canonical fade phenomenon might be surprising, it follows intuitively from understanding that the scintillation signal resides in the complex plane. The signal can be said to wander around in the complex plane with a velocity related to the decorrelation time τ_0, and the area over which it wanders is related to S_4. Every time the signal passes within a small neighborhood of the origin, the amplitude approaches zero, corresponding to a deep fade. At the same time, the phase changes rapidly by approximately $180°$ or half a cycle. Figure 1 illustrates this idea with a short segment of empirical scintillation power and phase data in Figure 1a, and the first three seconds of the same data plotted in the complex plane in Figure 1b. The statistical model presented here preserves realistic canonical fades in its generated scintillation histories. Phase screen-generated scintillation also contains canonical fades, but several previous statistical models have apparently generated phase and amplitude independently and thus produced unrealistically mild scintillation [6,11].
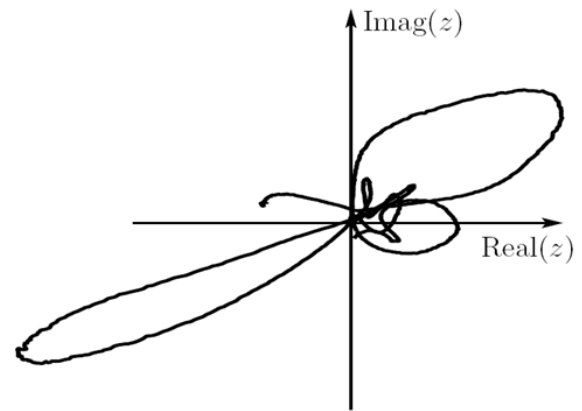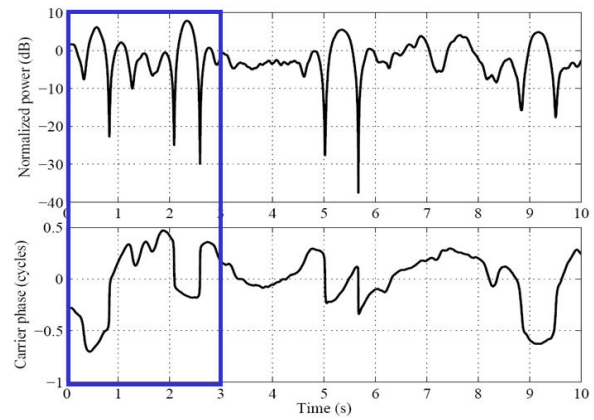

Figure 1. (a) Empirical amplitude and phase scintillation history containing several "canonical fades". (b) The same scintillation data plotted in the complex plane.

Figure 2 shows a segment of statistical generated scintillation data containing canonical fades. The scintillation indices ($S_4 = 0.9$, $\tau_0 = 0.4$) have been chosen to approximately match those of Figure 1 and thus demonstrate the qualitative similarity of this generated scintillation to the empirical scintillation in Figure 1a.
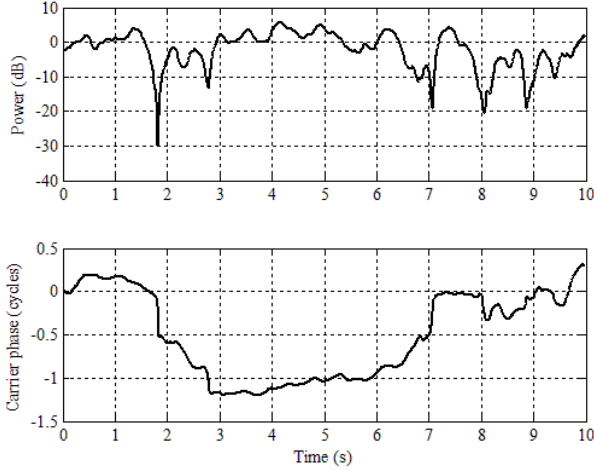
Figure 2. Synthetic amplitude and phase scintillation history generated by statistical model.

If one is to preserve canonical fades in generated time histories of scintillation, amplitude and phase cannot be treated as independent quantities. Instead, the signal must be analyzed in its complex form. For PLL tracking purposes, it is sufficient to model the phase and amplitude changes in a tracking channel as the sum of a complex constant $\bar{z}$, known as the direct component, and a time-varying complex fading process $\xi(t)$:

$$z(t) = \bar{z} + \xi(t) \qquad (1)$$

Reference [12] demonstrates experimentally that $S_\xi(f)$, the power spectrum of $\xi(t)$, can be approximated by the frequency response of a 2nd-order Butterworth filter. The bandwidth of this filter is related to τ_0, the decorrelation time of $\xi(t)$, by

$$B_d = \frac{\beta}{\sqrt{2\pi\tau_0}} \qquad (2)$$

where $\beta = 1.2396464$, a constant. Similarly, the amplitude distribution of the entire scintillation signal $z(t)$ can be modeled by a Rice distribution with the Rician K parameter related to S_4 by

$$K = \frac{\sqrt{1-S_4^2}}{1-\sqrt{1-S_4^2}} \qquad (3)$$

To compose discrete time histories of $z(k)$ with the specified amplitude distribution and autocorrelation function, one first creates a discrete time history $\tilde{z}(k) = \tilde{\bar{z}} + \tilde{\xi}(k)$ at a higher sampling frequency to act as an approximation of the continuous-time signal. The fading process $\tilde{\xi}(k)$ is implemented by passing zero-mean

complex white Gaussian noise through a 2nd-order Butterworth filter with a bandwidth specified by Eq. (2). To this is added the direct component $\tilde{\bar{z}}$, which relates to the Rician K of Eq. (3) according to

$$\tilde{\bar{z}} = \sqrt{2\sigma_\xi^2 K} \qquad (4)$$

where σ_ξ^2 is the variance of the previously created fading process. The combined quantity $\tilde{z}(k)$ must then be appropriately normalized so that $E[|\tilde{z}(k)|^2] = 1$. Finally, one constructs the discrete-time series $z(k)$ by averaging the samples in the continuous-time approximation over the desired discrete sampling interval.

III. HARDWARE-IN-THE-LOOP IMPLEMENTATION AND CAPABILITIES

Several steps are required to implement scintillation robustness evaluations in a hardware-in-the-loop configuration. The first and most complicated of these is to generate realistic histories of scintillation, as described in Section II. The remaining parts of the procedure are specific to the hardware platform chosen. For this paper, a Spirent GSS7700 GPS signal simulator was employed, along with Spirent's SimGen software. Figure 3 gives an overview of the implementation steps.
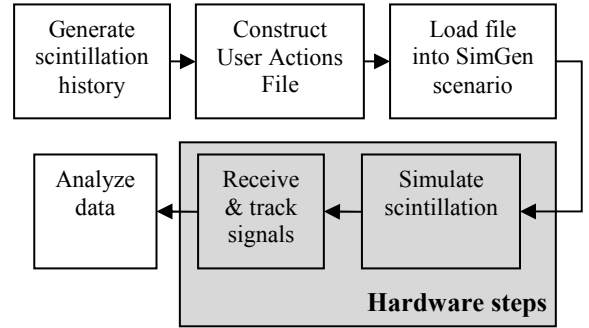

Figure 3. Hardware-in-the-loop implementation diagram.

A GPS signal simulator such as the Spirent GSS7700 allows the user to create a "scenario"; this includes specifying the time, simulated receiver location, satellites present and satellite orbits, signal power, and other details relevant to the simulation. In order to simulate ionospheric scintillation, the user must also be able to input a time series of modifications to the signal amplitudes and phases at a relatively high frequency. This was accomplished via a built-in capability known as a User Actions File.

A User Actions File allows some changes to be applied mid-scenario by use of timestamped command lines. MOD, one of the available commands, implements a modification to the signal level, phase range, or pseudorange of a specified signal. To generate simulated scintillation, one constructs a User Actions File containing a series of single-line MOD commands, each of which applies a single phase offset and amplitude offset pair from the previously created history of scintillation. The command syntax requires that the signal level modification be given in units of dB, and the phase range modification be given in units of meters. Timestamps identify the time relative to the start of the scenario at which the modification is to be applied. For the Spirent GSS7700, the update rate may be as high as 100 Hz, provided this setting is enabled in the hardware. This rate is sufficient for even quickly-varying scintillation (for instance, with $\tau_0 = 0.2$ seconds).

Considerable flexibility is built into the command line syntax. The user may specify not only the time and nature of the signal offset, but also the satellite PRN number to which the offset is to be applied, the frequency (i.e. L_1, L_2, etc.) and even the GNSS signal type, if the simulator is capable of producing more than one type of signal. By combining these capabilities and writing more than one command line per time interval, multiple satellites can be made to scintillate independently on multiple frequencies. For instance, if a receiver test required four satellites with both L_1 and L_2 scintillation over a period of 300 seconds with 10 millisecond updates, the User Actions File would contain 4 x 2 x 300 x 100 = 240,000 command lines, eight for each unique timestamp.

These options have been automated in a MATLAB function named genUAF.m. It takes as inputs the complex generated scintillation histories (one per satellite per frequency), the time history at which the modifications are to be applied, the PRN numbers of the scintillating satellites, and the length of time into the scenario before the scintillation event commences. Generally, the scenario should run for 1-5 minutes prior to the onset of scintillation to ensure that the receiver being evaluated has had sufficient time to acquire all satellites. The function asks the user to input the name of the User Actions File, which must have a .cmd extension. Manual editing of the created file can be performed in a text editor.

After creating a User Actions File with the desired scintillation data, receiver evaluation is straightforward. The receiver's RF input is connected to the simulator's output, and the receiver is configured for data logging. The user saves the User Actions File in the folder that contains the relevant SimGen scenario. Within SimGen, one loads the scenario, and finds "User actions file" under the scenario's "Options" settings. The file can be loaded by right-clicking and selecting it from a list of available files. Figure 4 shows this portion of the scenario menu. When the user runs the scenario, the selected User Actions File automatically performs the necessary signal modifications at the correct times.
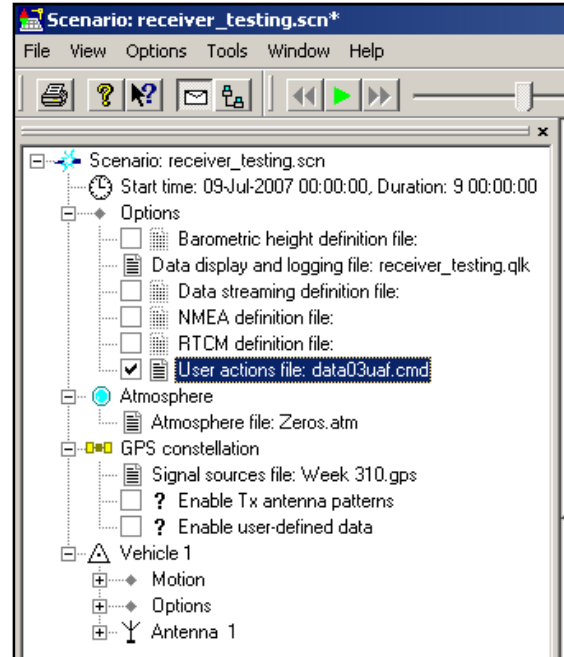

Figure 4. "User Actions File" option in SimGen menu.

IV. RESULTS OF VALIDATION, PERFORMANCE, AND NAVIGATION TESTS

Three types of tests were performed with the hardware-in-the-loop scintillation simulator. The first aimed to validate the operation of the hardware-in-the-loop setup; specifically, it investigated whether the amplitude and phase modifications loaded into the SimGen scenario were faithfully reproduced in the simulator RF output. Note that validation of the scintillation model itself was previously conducted [12]. The second set of tests explored the performance of four different receivers over a range of different scintillation severities. The third set of tests examined the degradation in the navigation solution with an increasing number of scintillating satellite channels.

A. Validation test

The goal of the validation test was to verify that the amplitude and phase variations output by the simulator matched those originally generated in software. The Cornell GNSS Receiver Implementation on a DSP (Cornell GRID receiver) was connected to the simulator,

and the signal amplitude and phase were logged at 100 Hz. Of the four receivers tested, only the Cornell GRID receiver was capable of logging raw phase measurements and able to observe at the 10-millisecond update rate commanded in the User Actions File. Some post-processing was necessary to remove the effects of satellite motion and clock drift from the phase measurements. The scenario employed an almanac from January 15, 2006, and a receiver location of 15° N latitude, 0° longitude, and 0 meters altitude. After two minutes of non-scintillating data, five minutes of scintillation were applied to PRN 27. Other degrading influences, such as ionospheric and tropospheric delay and multipath, were set to zero in the scenario.

Both the phase and amplitude measured by the receiver were very close to the originally generated values. Figure 5 plots the difference between the generated and measured C/N_0 and the generated and measured phase for a representative test case with $S_4 = 0.8$ and $\tau_0 = 0.2$. Except for occasional spikes, the difference in C/N_0 generally falls within the range of -1 to 1 dB-Hz. The phase also varies only slightly in most intervals, but it exhibits cycle slips from time to time so that the difference does not remain near zero over the whole data set.
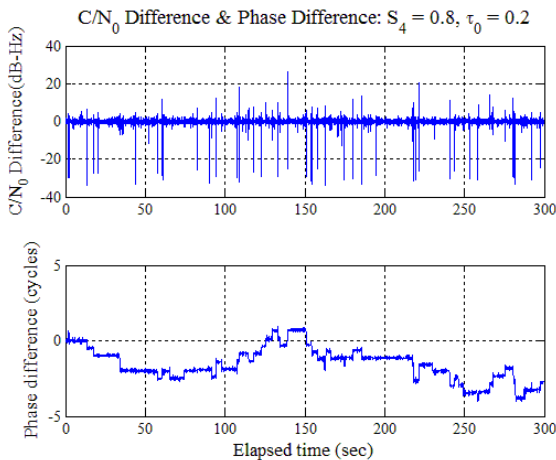

Figure 5. Amplitude and phase difference of generated and measured scintillation data.

Figure 6 displays the actual values of the phase and amplitude variations as generated and measured for only the first 30 seconds of the same data set. In the C/N_0 plot the generated signal is offset 20 dB-Hz above the measured value so the two can be distinguished, and likewise the generated phase is offset 1.5 cycles above the measured phase.
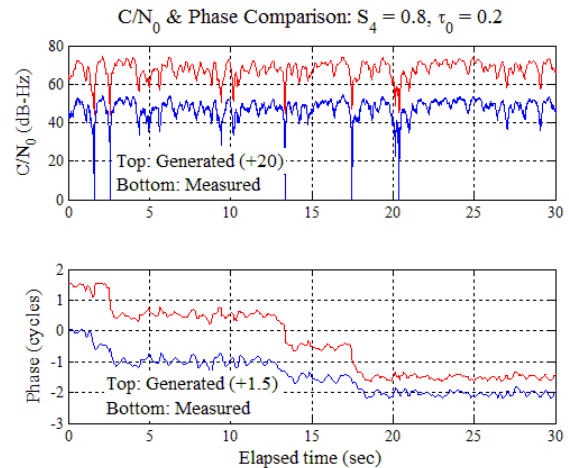

Figure 6. Comparison of generated and measured scintillation data.

B. Performance tests

Four different receivers were compared for performance during various scintillation events. The four receivers were the NovAtel ProPakII (OEM3 family), the GPS Silicon Valley GSV4004B Ionospheric Scintillation and TEC monitor, the Cornell GRID receiver, and the Magellan ProMark X. Each was evaluated over a matrix of different scintillation index pairs with S_4 values of 0.5, 0.8, or 1.0 and τ_0 values of 2.0, 0.5, or 0.2 – nine different combinations in all, ranging from mild to very severe scintillation. The scenario parameters were the same as in the validation test except for minor adjustments (for instance, the length of time prior to the onset of scintillation had to be increased for some of the receivers with longer acquisition times). Eight satellites were present, with only PRN 27 scintillating. In general, one might prefer to have only the scintillating satellite present to reduce noise as much as possible, but some receivers required a navigation solution in order to log data. As before, ionospheric and tropospheric delay and multipath were excluded. No two receivers shared data logging rates or observables, and this made comparison difficult. In each case, data were logged at the highest possible rate for that receiver, and observables were chosen to be as similar as possible to signal amplitude and phase. In addition, an attempt was made where possible to estimate the number of cycle slips over the five-minute interval, or to estimate some other related indicator of phase tracking performance such as the number of phase anomalies detected or the number of times the receiver reported losing lock on the signal. These quantities were compared with the predicted number of cycle slips for the given S_4, τ_0, and C/N_0, determined by the method described in Reference [3].

The NovAtel ProPakII logged data at a rate of 4 Hz. The two quantities recorded were C/N_0 and "lock time", a

measure of the time elapsed since the receiver regained lock on the signal. Whenever lock time reset to zero, the receiver was said to have lost lock. What exactly was meant by "lock" in this case was not determined. Very possibly the receiver could experience cycle slips without fully losing lock, so a count of how many times this occurred might underreport cycle slips. On the other hand, the relatively slow data rate (25 times slower than the simulator update rate) suggests that some "lost lock" events might occur several times between data points and only be logged as one event. Table 1 summarizes the performance results over the matrix of scintillation indices. For each combination of S_4 and τ_0, two quantities are given. The non-underlined quantity is the number of times the receiver reset its lock time value during the five-minute interval. The underlined quantity is the approximate number of cycle slips expected for that scintillation level. In the table, scintillation severity increases from top to bottom and from left to right. The measurements indicate as expected that as the severity of the scintillation increased, the lock time reset to zero more frequently.

Table 1. NovAtel ProPakII performance summary.

Loss of lock/ Predicted cycle slips		τ_0		
		2.0	0.5	0.2
S_4	0.5	0/0	0/0	1/0
	0.8	17/7	39/11	56/30
	1.0	59/13	75/30	83/115

Two representative data sets from the table are given in Figures 7 and 8. These correspond to the double-outlined boxes in Table 1. Figure 7 shows the data for the $S_4 = 0.8$, $\tau_0 = 2.0$ case of moderately severe scintillation, and Figure 8 shows the $S_4 = 1.0$, $\tau_0 = 0.2$ case of very severe scintillation. The upper half of each plot displays C/N_0, with the generated C/N_0 offset above it, and the lower half of each plot displays lock time. Comparison of Figs. 7-8 indicates that the receiver had more difficulty maintaining lock during more severe scintillation; furthermore, it less accurately tracked C/N_0 when the variations in that quantity were more rapid.
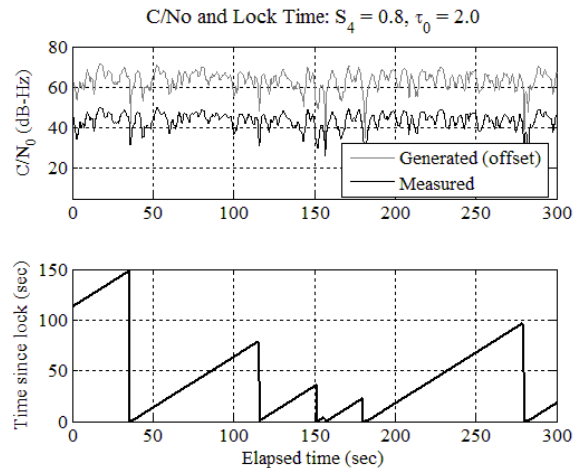

Figure 7. NovAtel performance during moderately severe scintillation; good C/N_0 tracking and occasional lock time resets.
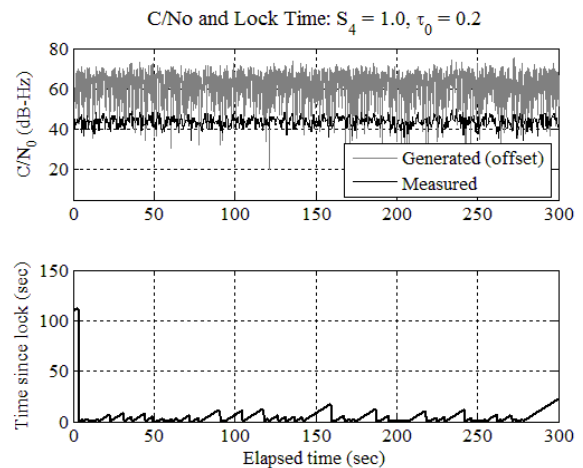

Figure 8. NovAtel performance during very severe scintillation; poor C/N_0 tracking and frequent lock time resets.

The GSV4004B was capable of logging data at 50 Hz. It reported a measure of signal power proportional to C/N_0 and an accumulated phase range in units of cycles. The phase range would ramp up (or rather down, as it became more negative) over time but reset to zero whenever a phase anomaly was detected. Thus a count of phase anomalies during the five-minute interval was obtained. Not every phase anomaly large enough to be detected would result in a cycle slip, so the phase anomaly count would be expected to exceed the cycle slip estimate. Some difficulty arose in the counting of phase anomalies when the phase range stayed near zero for several 20-millisecond intervals before decreasing. In this situation, it was unclear whether only one event or several in a row had occurred. In Table 2 the test results are given. The underlined quantity is the predicted number of cycle slips

as in Table 1, and the non-underlined quantity is the phase anomaly count, which slightly exceeds the predicted number of cycle slips as expected.

Table 2. GSV4004B performance summary.

Phase anomalies/ Predicted cycle slips		τ_0		
		2.0	0.5	0.2
S_4	0.5	0/0	0/0	0/0
	0.8	10/9	25/13	54/32
	1.0	21/17	52/33	175/120

Figures 9 and 10 show the measured data for the double-outlined table entries. The signal power matched the generated history better than the NovAtel receiver for both cases, in part because of the higher logging rate. For the more severe scintillation case, the accumulated phase reset to zero often.
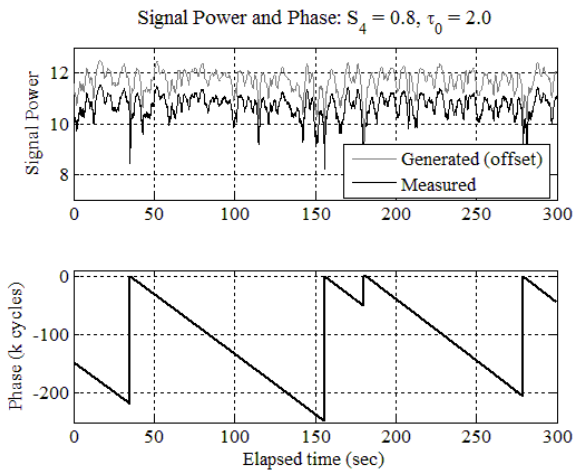

Figure 9. GSV4004B performance during moderately severe scintillation; occasional phase anomalies detected.
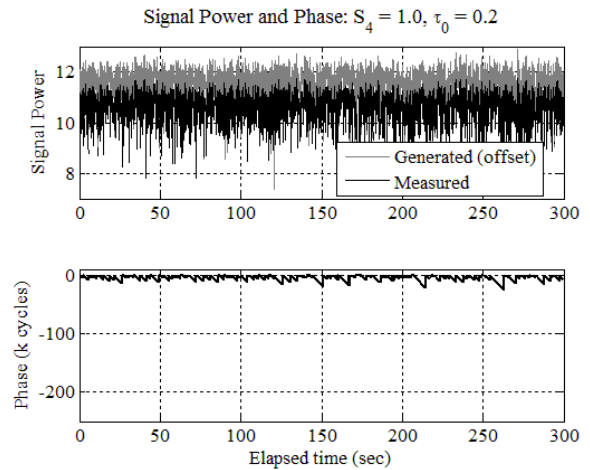

Figure 10. GSV4004B performance during very severe scintillation; frequent phase anomalies detected.

With the Cornell GRID receiver, 100 Hz logging was possible and both amplitude and phase measurements could be determined after some post-processing. Consequently, cycle slips could be counted by examining a plot resembling the lower half of Figure 5, and these could be directly compared to the predicted cycle slip estimate. Table 3 summarizes the results of this data analysis. For most cases, the number of cycle slips measured was larger than that predicted, but of the same order of magnitude.

Table 3. Cornell GRID receiver performance summary.

Cycle slips/ Predicted cycle slips		τ_0		
		2.0	0.5	0.2
S_4	0.5	0/0	0/0	0/0
	0.8	2/3	10/7	51/25
	1.0	6/6	36/23	199/107

The C/N_0 tracking for the Cornell GRID receiver was the most accurate observed for any of the four, but this is likely due in part to its higher logging rate. Figures 11 and 12 are similar to Figures 7-8 and 9-10, except that the lower half of each plot shows the difference between true and measured phase like the lower half of Figure 5.
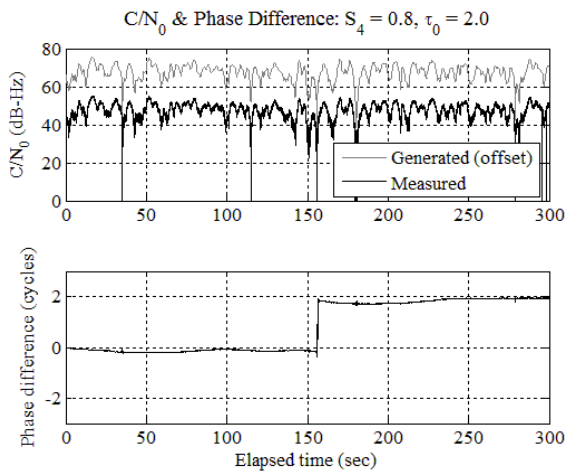
Figure 11. Cornell GRID receiver performance during moderately severe scintillation; few cycle slips.
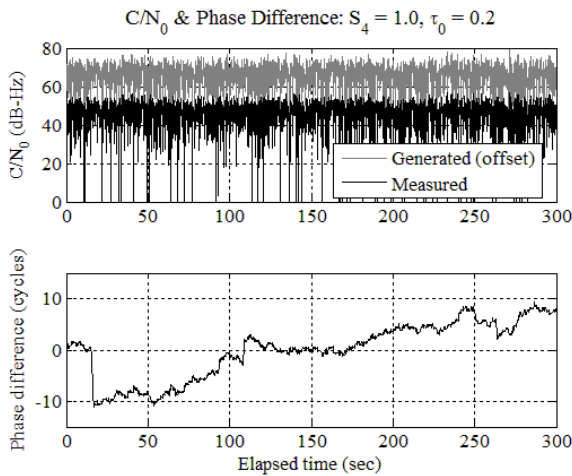

Figure 12. Cornell GRID receiver performance during very severe scintillation; frequent cycle slips.

The Magellan ProMark X is a handheld receiver more than a decade old, so it was not expected to perform as well as a newer model intended for research. Its maximum logging rate was only 1 Hz. Instead of C/N_0 it reported "signal quality", a discrete value ranging from 0 to 9 and corresponding roughly to signal strength. According to the documentation, a signal quality of 3 or less could result in loss of lock on a given channel. The Magellan also reported an accumulated phase range similar to that reported by the GSV4004B, which set itself to zero whenever sufficient tracking problems occurred. Unlike that receiver, however, the Magellan's phase measurement reset to something near its old value after a time if the scintillation was not too severe. Even when the phase reading was zero, the receiver logged pseudoranges and signal quality measurements successfully. This evidence suggests that it continues tracking with a delay lock loop (DLL) when the PLL fails.

Table 4 summarizes the test results, but it differs somewhat from the previous tables. Because the receiver did not measure C/N_0, the expected number of cycle slips could not be predicted by the same algorithm. Furthermore, phase anomalies did not occur as discrete events and thus could not be counted. As a substitute, the table reports the percentage of the five-minute scintillation interval during which good phase measurements were unavailable. Surprisingly, the performance according to this metric actually improved when going from $\tau_0 = 0.5$ to $\tau_0 = 0.2$ with S_4 constant at 0.8. The slow logging rate might account for this apparent improvement, or the percentage measurement might not accurately represent true receiver performance. A better understanding of the receiver's tracking strategy would be necessary to resolve the discrepancy.

Table 4. Magellan ProMarkX performance summary.

Percent of time without phase measurement		τ_0		
		2.0	0.5	0.2
S_4	0.5	0	0	0
	0.8	4	46.7	29
	1.0	24.7	62.7	87.3

Figures 13-14 plot the data for the two double-outlined entries as in previous figures. For the more severe case, Figure 14 indicates that phase measurements were completely unavailable for the majority of the data set.
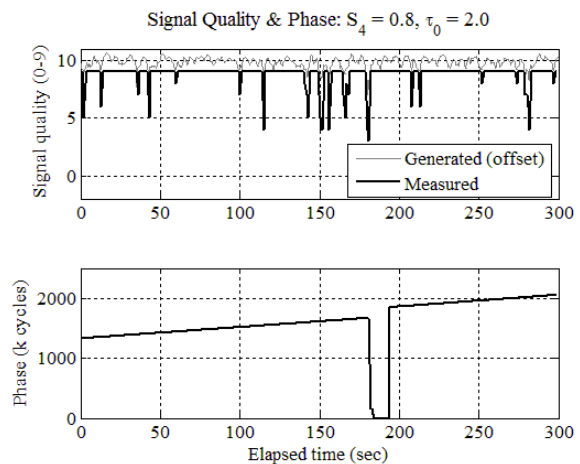

Figure 13. Magellan performance during moderately severe scintillation; some phase data unavailable.
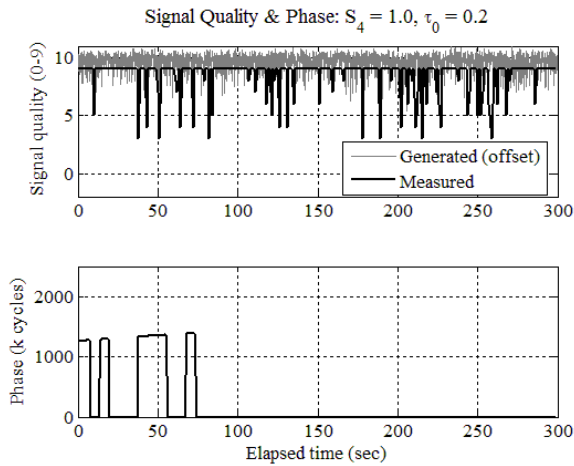
Figure 14. Magellan performance during very severe scintillation; most phase data unavailable.

C. Navigation tests

A third set of tests looked at the effects of scintillation on navigation solution accuracy, in this instance for the NovAtel ProPakII. The purpose was not to test the solution accuracy of a particular receiver but rather to explore the range of evaluation possibilities offered by the scintillation simulator. The relatively severe scintillation index set ($S_4 = 1.0$, $\tau_0 = 0.5$) was chosen, and the same basic scenario with eight satellites present was used. In each successive test, the number of scintillating satellites was increased by one. The order in which the satellites were made to scintillate was random. Five minutes of position data were collected, and compared to the true (simulated) position.

Table 5 summarizes the navigation test results. In addition to the RMS 3D position error over the five-minute interval, it lists the geometric dilution of precision (GDOP) that would exist if all scintillating channels were removed from the calculation. Unexpectedly, the position errors actually decreased initially as the first few signals started to scintillate. The apparent cause is that some of the errors added to the solution partially canceled those that were present at first.

Table 5. Results of navigation solution tests.

Number of scintillating satellites	GDOP w/o scintillating satellites	RMS 3D position error (m)
0	1.922	5.077
1	1.982	5.001
2	2.248	4.960
3	2.406	4.908
4	7.858	6.166
5	N/A	7.079
6	N/A	8.814
7	N/A	8.925
8	N/A	8.706

Figures 15-17 display the horizontal position errors over the five-minute interval for the cases of 0, 4, and 8 scintillating signals. Satellite geometry appears to strongly influence the error spread, suggesting that the main effect for this test was in the different sets of satellites used to compute a solution. In other words, as the scintillating signals dropped out, the geometry of the remaining satellites determined the directions in which the errors increased most significantly.
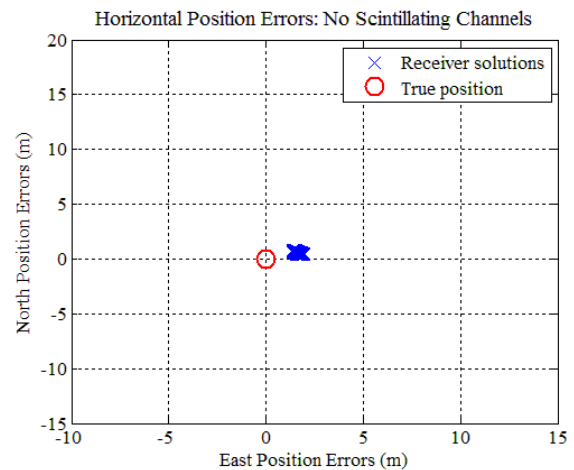

Figure 15. Horizontal position errors with no scintillating satellite channels (initial case).
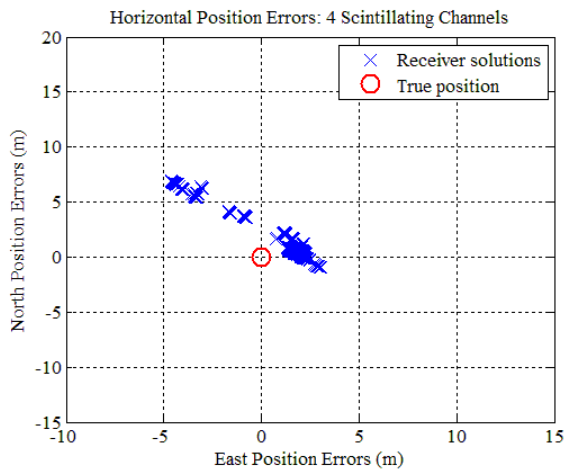
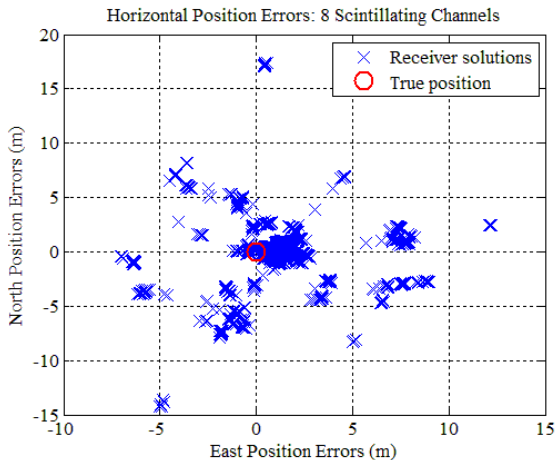Figure 16. Horizontal position errors with 4 scintillating satellite channels.

Figure 17. Horizontal position errors with 8 scintillating satellite channels.

V. CONCLUSIONS

A hardware-in-the-loop technique has been implemented that is able to evaluate the robustness of GPS receivers during ionospheric scintillation. It employs a simple statistical scintillation model that accurately reproduces the characteristics of empirical scintillation most significant for receiver tracking loop performance. Histories of modeled scintillation are incorporated in the output of a GNSS signal simulator.

The range of tests completed demonstrates the flexibility of the method, which allows the tester to define receiver performance in many different ways. This strength, however, has a corresponding weakness: comparison between different receiver models is hindered by the lack of common standards, especially in logging rates and observables. Receiver development would benefit from a

standard performance metric for scintillation robustness. Nevertheless, the hardware-in-the-loop method presented here provides a simple yet powerful tool for developing GNSS receivers that are more robust to ionospheric scintillation.

REFERENCES

[1] Kintner, P. M., Jr. and B. M. Ledvina, "The ionosphere, radio navigation, and global navigation satellite systems," *Advances in Space Research*, vol. 35, no. 5, pp. 788–811, 2005.

[2] Humphreys, T. E., M. Psiaki, B. Ledvina, A. Cerruti, and P. M. Kintner, Jr., "A data-driven simulation testbed for evaluating GPS carrier tracking loops in severe ionospheric scintillation," *IEEE Transactions on Aerospace and Electronic Systems*, in revision after favorable reviews.

[3] Humphreys, T. E., M. Psiaki, B. Ledvina, A. Cerruti, and P. M. Kintner, Jr., "Modeling the effects of ionospheric scintillation on GPS carrier phase tracking," *IEEE Transactions on Aerospace and Electronic Systems*, in revision after favorable reviews.

[4] Skone, S., G. Lachapelle, D. Yao, W. Yu, and R. Watson, "Investigating the impact of ionospheric scintillation using a GPS software receiver," in *Proceedings of ION GNSS 2005*, Long Beach, CA: Institute of Navigation, Sept. 2005.

[5] Morrissey, T. N., K. W. Shallberg, A. J. Van Dierendonck, and M. J. Nicholson, "GPS receiver performance characterization under realistic ionospheric phase scintillation environments," *Radio Sci.*, vol. 39, pp. 1–18, 2004.

[6] Groves, K. M., S. Basu, J. M. Quinn, T. R. Pedersen, K. Falinski, A. Brown, R. Silva, and P. Ning, "A comparison of GPS performance in a scintillating environment at Ascension Island," in *Proceedings of ION GPS 2000,* Institute of Navigation, 2000.

[7] Humphreys, T. E., M. L. Psiaki, B. M. Ledvina, and P. M. Kintner, Jr., "GPS carrier tracking loop performance in the presence of ionospheric scintillations," in *Proceedings of ION GNSS 2005,* Long Beach, CA: Institute of Navigation, Sept. 2005.

[8] Forte, B. and S. M. Radicella, "Comparison of ionospheric scintillation models with experimental data for satellite navigation applications," *Annals of Geophysics*, vol. 48, no. 3, pp. 505–514, June 2005.

[9] Conker, R.S., M. B. El-Arini, C. J. Hegarty, and T. Hsiao, "Modeling the effects of ionospheric scintillation on GPS/Satellite-Based Augmentation System availability," *Radio Science*, vol. 38, pp. 1–1, Jan. 2003.

[10] Strangeways, H. J., V. E. Gherm, and N. N. Zernov, "Modeling and Mitigation of the Effect of Scintillations on GPS," in *Proceedings of 49th International Symposium ELMAR-2007*. Zadar, Croatia: Sept. 2007.

[11] Hegarty, C., M. B. El-Arini, T. Kim, and S. Ericson, "Scintillation modeling for GPS-wide area augmentation system receivers," *Radio Science*, vol. 36, no. 5, pp. 1221–1231, Sept. 2001.

[12] Humphreys, T. E., M. Psiaki, and P. M. Kintner, Jr., "Simulating ionosphere-induced scintillation for testing GPS receiver phase tracking loops," IEEE Journal of Selected Topics in Signal Processing, in review.